

# Model fire tests on a beam-to-leg connection in an offshore platform topside

S. A. Hosseini<sup>1,\*</sup>, M. Zeinoddini<sup>1</sup>, A. Saedi Daryan<sup>1</sup> and M. Rahbari<sup>2</sup>

<sup>1</sup>*Civil Engineering Department, Khajeh Nasir Toosi University of Technology, Tehran, Iran*

<sup>2</sup>*Iranian Offshore Engineering and Construction Company, Tehran, Iran*

## ABSTRACT

Beam-to-column connections are of great significance as they noticeably influence the mechanical behavior of structures at ambient and elevated temperatures. Observations from full-scale fire tests confirm that connections play an important role on the resistance time of structural components in fire. Because of the high cost of elevated temperature tests, adequate experimental data on a broad range of connections are not available. One type of such connections is the I-beam-to-circular tubular leg connections in offshore oil/gas platform topsides. Considering the high risk of fire events in offshore oil/gas platforms, our study focuses on the structural behavior of this type of connection at elevated temperatures. Eleven small-scale experimental tests were conducted on a uniplanar welded steel I-beam-to-tubular chord connection with external diaphragms to investigate their fire resistance capacity. Local strengthening and partial thermal insulating were separately introduced to the connection components. The results show that the external diaphragms play a considerably more important role on the connection fire response as compared with that for the vertical stiffeners. It is also found that the degradations in the connections' stiffness at elevated temperature might be closely correlated with the classical thermomechanical data on steel material. Copyright © 2013 John Wiley & Sons, Ltd.

Received 28 November 2012; Revised 11 June 2013; Accepted 12 June 2013

**KEY WORDS:** I-beam-to-circular tubular leg connection; steel oil/gas platforms; topside; elevated temperature; rotation–temperature curve; fire; experimental study; external diaphragms

## 1. INTRODUCTION

### *1.1. Connections in steel offshore platforms*

Topsides of the offshore platforms are often provided with portal or truss-type structures. The truss usually consists of I-beams as chords and tubulars as diagonals. The hot rolled or welded I-beams (chords) need to be connected to the main legs of the platform, which are piercing up the sea from the substructure. For secondary topside joints or for lighter loaded truss structures, unstiffened I-beam-to-tubular connections have been successfully used. For the main joints of heavy topsides, I-beam-to-tubular leg connections with external diaphragms are usually employed [1, 2]. These connections are the key structural elements in the topside structure of the oil/gas platforms [3]. With this connection, the shear loads are transferred by the web plates welded to the tube wall. The moment is transmitted by the diamond plates in combination with an effective ring width of the tubular 'can'. A view of the topside of an offshore platform in a fabrication yard is shown in Figure 1. An I-beam-to-tubular connection with external diaphragms is highlighted in the figure.

\*Correspondence to: S. A. Hosseini, Civil Engineering Department, Khajeh Nasir Toosi University of Technology, Tehran, Iran.

†E-mail: hosseini@dena.kntu.ac.ir

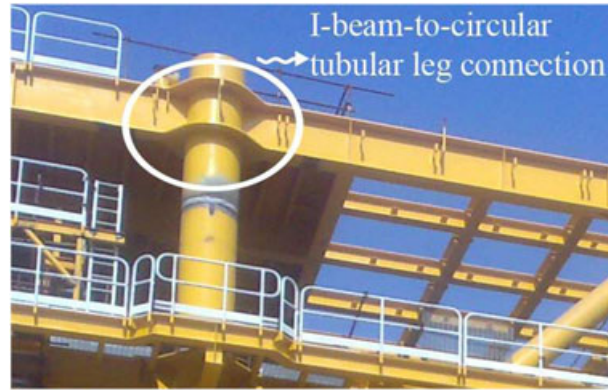


Figure 1. A view of a typical I-beams-to-tubular connection, with external diaphragms, in oil offshore platform topside.

### 1.2. Fire events in offshore oil/gas platforms

Hydrocarbon production from offshore facilities has grown fourfold in the last three decades [4]. The number of accidents also shows a surge. From 1980 to 2005, 7018 accidents are reported to have occurred in fixed offshore units [5]. Statistics presented in the worldwide offshore accident databank confirms that fire occurrence is one of the most detrimental causes of annual damage in steel oil platforms [6]. Figure 2 shows a photo of a fire accident in an offshore oil platform.

During the past four decades, more than 60 major fire accidents have been reported on offshore oil/gas platforms [7]. The total number of platforms of various types that have been installed worldwide exceeds 10,000 units [8]. Fire accidents in offshore facilities can lead to partial or total collapse or sinking of an offshore platform with serious consequences including the loss of lives, the destruction of properties, and damages to the environment [9]. Some examples of major fire accidents are summarized in Table I [10]. The table gives the location of the facility, the accident time, the causes, and the losses.

Thus, accidental fires are a continuous threat for offshore hydrocarbon structures, and it is vital to ensure that an offshore oil and gas structure is properly designed to minimize the postaccident consequences if a fire does happen to the structure.

### 1.3. Behavior of the I-beam-to-tubular leg connections at elevated temperatures

The National Institute of Standards and Technology, which has published the results of its investigation of the World Trade Center disaster, identifies structural connections under fire



Figure 2. A fire event in an offshore oil platform.

Table I. Major accidents on offshore oil/gas platforms [10].

Number	Facility name and location	Year	Causes of fire	Losses
1	Ekofisk, Norway	1975	Blowout and oil riser failure resulted in major fire	Six dead
2	Piper Alpha, North Sea, UK	1988	Gas leak resulted in explosion	167 dead and \$3bn loss
3	Mobil Oil Rig, Nigeria	1995	Explosion of oil rig	13 dead
4	Morgan oil field, Gulf of Suez, Egypt	1996	Explosion of oil rig	Three dead and two injured
5	Esso, Longford, Victoria, Australia	1998	Human error in gas production plant	2 dead and \$1.3bn loss
6	Glomar, Arctic IV, Invergerdon, UK	1998	Explosion in rig	Two dead
7	Gabriel Passos Refinery, Minas Gerais, Brazil	1998	Fire	Three dead
8	Petrobras, Brazil	2001	Explosion in platform	10 dead and \$430m loss
9	High North Platform, Bombay	2005	Massive fire in process platform	22 dead
10	Kab Field, Bay of Campeche, Gulf of Mexico, USA	2007	Strike in the production platform causing riser release and fire	22 dead and 5000 bbl oil lost
11	Apache platform in the Gulf of Mexico, USA	2010	Fire	One dead

exposures as a vital area for further study [11]. Very few fire tests were conducted on assemblies with real end connections, in place of the common insertion of the assembly frame into the furnace. Most assemblies typically had simple bearing supports butted against the test frame for floors and roofs, or to the load device for walls [12].

Considering the importance of connection performance in steel structures in fire condition, some experimental and numerical studies were carried out to investigate the behavior of connections in onshore steel buildings [13–19]. However, the number of studies about the behavior of connections of offshore platforms is very limited. Previous studies on fire in offshore platforms mainly deal with the risk assessment [20, 21], reliability analysis [22, 23], analytical modeling [23, 24], numerical simulation [25–27], and general topics [20,25] related to the offshore structures exposed to fire. The authors are not aware of any previous study on the behavior of I-beams-to-tubular connections with external diaphragms in fire or fire experiments on offshore structures connections.

#### 1.4. Scope and objectives of the current study

Considering the aforementioned points, this study addresses the behavior of offshore oil platform topsides in fire. A complex offshore structure contains a large number of structural elements and details. In the present paper, focus is set on the behavior of the welded I-beams-to-tubular connections with external diaphragms. It has been tried to find out how this type of joint behaves at elevated temperatures. An experimental approach was considered.

## 2. EXPERIMENTAL TEST DESIGN AND SPECIMENS

### 2.1. Test specimens

Specimens considered in the current study represent a typical I-beam-to-tubular-leg connection in the topside of a steel offshore jacket platform. The specimens were constructed to 1/8 scale of an existing connection in the main deck of one platform in the South Pars gas field in the Persian Gulf. It is acknowledged that the connection demonstrates a highly nonlinear response in fire. Enough care has to be taken in extrapolating the results from 1/8 scale to 1 scale. Wang *et al.* [28] suggested that, when conducting fire tests on small-scale models, the temperature of the compartment fire would be independent of scale. The temperature inside a heated object, however, will inherently depend on

the scale because of the dependence on geometry (e.g., thickness of insulation) and thermal properties (e.g., conductivity). With an unprotected steel structure, it might be, therefore, assumed that the steel temperature is proportional to the furnace temperature (and so independent of scale). This might not be essentially true for a thermally insulated structure.

In the current study, all specimens, except specimens S8 and S9, were unprotected. Specimens S8 and S9 were included partial thermal insulating. This, as will be discussed in the succeeding texts, was not aimed at modeling a full-scale condition but to merely substantiate the thermal/mechanical role of different components in the connection on the overall fire performance of the connection. Independency to the scaling, therefore, might not be specifically applicable to these two specimens. The succeeding scaling rules, when applicable, can be considered for possible extrapolation of the test results to the full scales:

$$t \sim s^{1/2} [28] \quad (1)$$

$$F \sim s^2 [29] \quad (2)$$

$$M \sim s^3 [29] \quad (3)$$

where  $s$  is the length scale,  $t$  is the time, and  $F$  and  $M$  are force and moment, respectively. It should be noted that in the current study, only a simple geometric scaling of the specimens was considered. The specimens' geometry was 1:8 of a real connection in an existing offshore topside platform (including beam, column, stiffeners, diaphragms, and welds sizes). The mechanical properties for the steel and weld materials remained almost the same. The theoretical connection capacity at room temperature reported in the paper was for the small-scale specimens. The scaling rules mentioned in the preceding texts allow test data derived from the specimen geometry to be extrapolated to real structures. This was not conducted in this paper for brevity.

All the specimens were configured to form a uniplanar T-shaped assembly with a single rolled I-section beam welded to one side of a circular tubular column through external diaphragms. The connection details can be subdivided into several parts. The column was a seamless steel tubular, 100 cm long of grade X52. It had an outer diameter of 219.1 mm and a wall thickness of 12.7 mm. The I-beam was a 75-cm-long rolled steel IPE220, grade S355. The external diamond-type diaphragms and vertical stiffeners (Figure 3) had been fabricated from steel rolled plates grade S355. The plates were cut into the desired geometries using a computer numerically controlled cutting machine. The edges were machine beveled, where necessary.

Standard coupon tests were performed on samples extracted from the primary structural assembly members to determine their actual mechanical properties (including yield and ultimate strength, and elastic modulus). The results of the mechanical property tests are summarized in Table II.

The specimens were fabricated in the Iranian Offshore Engineering and Construction Company (IOEC) offshore-structure fabrication yard in Khoram Shahr, Iran, on the basis of the approved welding procedure specifications [30]. Two types of fillet welds and groove welds (with full penetration) were used in fabricating the specimens. The welding locations and types can be observed in Figure 3. All welds were made by qualified welders, using the shielded metal arc welding procedures, as per the given welding procedure specification. E7018 electrodes were used for the construction of the connection. Necessary care was taken to avoid distortions in the joint and in its interconnecting elements during the welding process. The specimens' dimensions were recorded before starting the tests.

The upper and lower beam flanges were groove welded to the corresponding external diaphragms. The two diaphragms also encircled the column and were groove welded to it. The beam web was welded to a vertical stiffener, which itself was welded to the column side. Three extra vertical stiffeners, with 90° spacing around the column circumference, were also weld mounted to the column wall and also to the upper and lower external diaphragms. The welds were subjected to post weld 100% visual inspection, dye penetrant, magnetic particle, and ultrasonic tests [31] at the

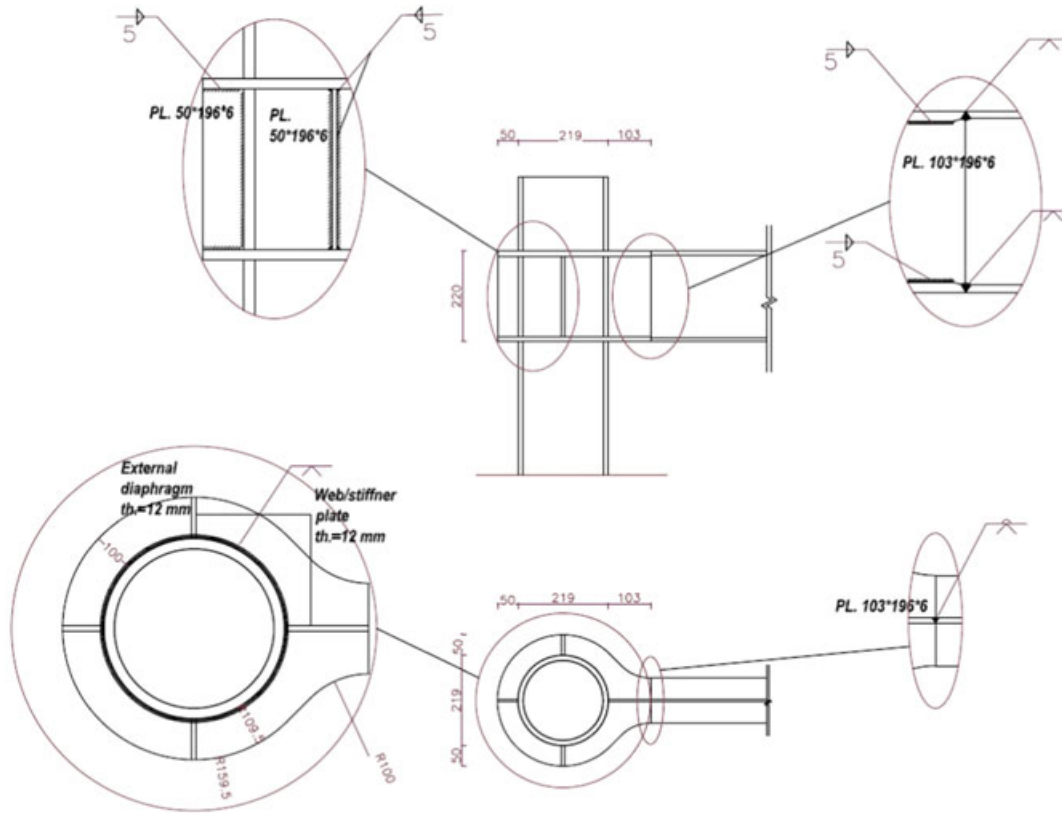


Figure 3. Details of the test specimens.

Table II. Material mechanical properties at room temperature.

Material	Steel grade	Yield stress (N/mm <sup>2</sup> )	Ultimate stress (N/mm <sup>2</sup> )	Modulus of elasticity (kN/mm <sup>2</sup> )	Charpy V-notch test (J)
I-beam	S355	352.7	490.4	205.8	—
Tubular column	X52	360.8	448.3	202.7	—
Plate, 15 mm thick	S355	353.5	492.6	202.4	—
Plate, 12 mm thick	S355	354.9	495.6	205.1	—
Plate, 8 mm thick	S355	355.2	493.2	203.3	—
Plate, 6 mm thick	S355	350.8	488.6	202.9	—
Weld metal	E7018	485.8	555.2	2.06	185

fabrication yard to assure the weld quality. They were also randomly examined by using radiography tests. Few trial specimens were also prepared for destructive examinations. They were sectioned for macrographic examination to ensure complete joint penetration and defect free joints. Figure 3 illustrates the details of the I-beam-to-tubular connection with external diaphragms.

## 2.2. Test setup

In order to demonstrate the performance of an I-beams-to-tubular connection with external diaphragms, the test setup showed in Figure 4 was employed. The tests were conducted in a gas-fired furnace, 120 cm long, 80 cm wide, and 80 cm high that was specifically designed for this study. Propane gas was used as the furnace fuel. A premixed automated burner was employed in the fire resistance furnace. Dimensional scaling principles were considered in the design of the test assembly

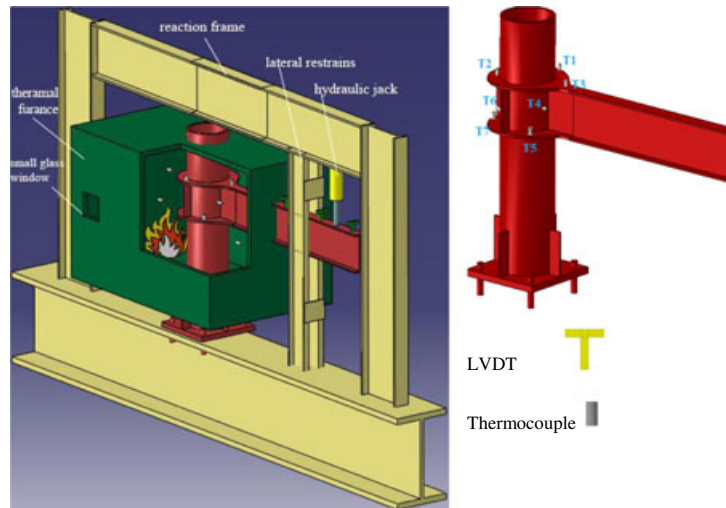


Figure 4. Schematic view of the test setup.

to represent the actual construction applications. The tubular column and the I-beam ends stayed outside the furnace.

The furnace construction was designed on the basis of the established principles of the fire resistance testing for the structural performance assessment [32]. All interior furnace surfaces were lined with one layer of 50-mm-thick ceramic fiber materials. The furnace structure was designed to avoid any obstruction to the free movement of the specimen under the imposed load and thermal actions. Tests were performed with a positive furnace pressure relative to the laboratory conditions across the entire test article.

The T-shaped specimen was supported by one fixed column end. The upper end of the tubular column and the far end of the I-beam had no restraint. For this, the column bottom was rigidly connected to a horizontal HPE 320 base beam (Figure 4). The column base connection capacity was sufficiently higher than the plastic flexural capacity of the steel tubular column. Vertical stiffeners were considered in the base beam at several locations, such as those below the column base (Figure 4).

The column upper end and the beam end had also no axial resistance. This means that the connection was examined under pure bending moments because of rotational constraint in the joint. The membrane action and the axial resistance effects on the joint behavior were, therefore, excluded in the tests. Lateral constraints were provided at two sides of the I-beam part of the specimen to ensure a uniplanar behavior. The constraints were preventing the specimen torsion but imposed no restraint for the in-plane movement of the I-beam.

In practice, a connection experiences a combination of in-plane, out-of-plane, and torsional deformations. However, in an experimental study, as the first of its kind, it would be very demanding to assess all these actions simultaneously. This also makes the interpretation of the results more complicated. The focus of the current study has, therefore, been on the uniplanar moment-rotation behavior of the connection. This is believed to be the dominant action in this type of connection. The out-of-plane and torsional deformations and their interactions with uniplanar deformations can be considered as part of a future study. The lateral restraints are shown in Figure 4, and they were designed to resist the maximum torsion moment of the beam.

### 2.3. Instrumentations

The instrumentations employed in the tests included Omega AC high-accuracy linear variable differential transformers (LVDTs, 150 mm stroke,  $0.2 \mu\text{m}$  resolution plus 100 mm stroke,  $0.1 \mu\text{m}$  resolution), a calibrated 100 kN load cell (Omega LCM1001 with operating temperature range of  $-46$  to  $100^\circ\text{C}$  and input/output resistance of  $350 \pm 10 \Omega$ ), thermocouples type K from Waltow, dual axis inclinometer sensors IS-2-30 from Level Developments (with accuracy of  $0.01^\circ$  and operating

temperature range of  $-25$  to  $85$  °C), an Enerpac 100 kN electronically controlled hydraulic jack, a TDS-303 data logger from TML, and a digital Sony video camera with a recording speed of 15 FPS.

A load cell was placed in series between the hydraulic jack and the I-beam to record and to monitor the magnitude of the applied load introduced throughout the test duration to the specimen. The time-history of the transverse deflections on two locations on the I-beam and on the far end of the column were recorded by using LVDTs. Plate thermometers were distributed across the test specimen surface and in the furnace to measure the temperature. During the tests, the temperatures were also measured on the unexposed sides of the test specimen with thermocouples placed on the specimen surface.

A small rectangular glass window, covered by a high temperature-resistant glass, was considered in one longitudinal side wall of the furnace (Figure 4). The window was placed in front of the connection panel in the specimen. It made it possible to acquire digital photos and videos from the specimen deformations during the tests and to monitor its lateral or torsional deflections. Subsequent image analysis provided valuable qualitative and quantitative deflection data.

A furnace calibration test was first conducted to quantify the thermal exposure onto a number of trial specimens in the absence and presence of applied loads. The thermal exposure calibration test data were used as a basis for the thermal exposure in all actual tests. This was to ensure a consistent, repeatable thermal condition and to minimize the effects of specimen construction on the exposure situation. Prior to initiation of the fire test, all structural instrumentation used in the test assembly were checked/calibrated under applied loads.

The furnace calibration test was aimed at prior calibrating of all test thermocouples and the data acquisition system. This was achieved by using a number of reference thermocouples, which themselves had up-to-date calibration certificates. The test thermocouples were placed within 50 mm of the reference thermocouples. Each calibration test was taking around 1 h, and the temperature varied from around  $20$ – $900$  °C. In addition, the burner control system and the repeatability of the furnace thermal performance were evaluated/calibrated. This was also conducted on the basis of readings from the reference thermocouples. In addition, the furnace calibration tests were giving indications on the maximum temperature at instrumentation locations. These tests were conducted on an uninstrumented specimen. This data was checked against thermal operation limits of different instrumentations prior to the main tests.

#### 2.4. Loading system

The tests proceeded in three steps. In the first step, in the room temperature, the specimen was subjected to a predefined applied load. The applied load introduced to the connections tested in this study was a combination of an in-plane moment plus shear, which was acting on the I-beam. These were the resultants of a concentrated vertical load, which was gradually imposed through a hydraulically controlled jacking system. The load magnitude was chosen as a fragment of the load representing the bending capacity of the connection. The load was introduced close to the far end of the I-beam. This part of the beam was intentionally left outside of furnace to keep the loading and measurement systems apart from direct heat. In these tests, the panel zone (in the connection) remained bare and directly exposed to fire. Other parts of the specimen, inside the furnace, were thermally insulated. The mechanical loading system was placed outside the furnace, therefore, the column and beam ends out penetrated the furnace wall. They remained uninsulated. Therefore, a heat sink effect was inevitable because of heat conduction directly from the hot part to the cold ends of the specimen. This accompanied a degree of heat loss. But, the effect was found not to be very significant. Maximum temperature at the far end of the beam, always, was less than  $50$  °C, whereas the temperature in the panel zone well exceeded greater than  $750$  °C.

The furnace wall, at the out penetration location of the specimen, was well-filled with ceramic fibers. They provided an effective fibrous thermal insulation while allowing for free deformations of the specimen during the tests. A load cell and three LVDTs at this part were used to record the load and the beam deflection, respectively. The applied load was kept constant during the next steps (2 and 3). A spherical thrust bearing was positioned between the upper flange of the I-beam and the shaft tip of the hydraulic jack. This arrangement ensured a friction-free contact mechanism and a self-alignment mechanism for the applied load, independent of the beam deflection during the test.

The second step started around 15 min past the full application of the applied load. The fire was started in the furnace, whereas the applied load to the specimens was kept constant. The furnace time–temperature exposure was gradually increased until the specimen failed under combined actions of the applied load and the elevated temperature. In this study, the ISO834 [33] standard temperature curve was adopted in operating the furnace. The ASTM E-119 [34] and ISO 834 [33] time–temperature curves are perhaps the most common furnace exposures used in fire resistance testing. It is, however, acknowledged that the UL 1709 [35] and EN 1363-2 [36] hydrocarbon fires could be considered for tunnel and offshore oil rig applications. These structures experience a more severe fire exposure than that for building applications. It is noted that all aforementioned exposure curves end in a gas temperature of 1100 °C. The UL 1709 reaches 1100 °C in 5 min. This is 27 min for EN 1363-2 and 180 min for ASTM E-119 and ISO 834.

Using a very rapid time–temperature curve was resulting in a very fast sequence of events during the fire tests. This was making the tracing of the mechanical events in the specimens and interpretation/comparison of the findings exceedingly difficult. The time–temperature curve used in the current study adopted the ISO 834 trend, while it reached 1100 °C in around 60 min.

Plate thermometers were used to measure the furnace temperature and to control the burner. It is noted that with all specimens, the column and beam surfaces were wrapped with a 2.5-cm-thick ceramic fiber blanket as thermal insulation. The fiber ceramic used was the production of DS Fibertech Corp., Lewisville city, Denton County, Texas, United States. The average thermal conductivity of the fiber ceramics was 0.15 W/mK. Only the connection zone (the panel zone areas, between the connection diaphragms) was exposed to the fire. This is because the objective of the current study was to investigate the fire response of the connections and its constitutive elements and details and not the interconnecting beams and columns. The previously mentioned arrangements represent the condition of a real connection in fire. Gravitational loads (weight of the structure and equipment) usually remain unchanged during the fire event, whereas the capacity of the structure gradually reduces.

A view of a specimen in furnace during the test is shown in Figure 5. In this figure, ceramic fibers on the top and bottom of the panel zone in column can be clearly observed. As it was mentioned, these fibers were protecting the areas outside the panel zone from a direct heat. It is noted that blanket-type materials are not common in offshore structures. In actual structures, passive insulation products, mostly sprayed fire-resistive materials, are used to envelope individual structural members. Some connections might remain without fire protection. In aging structures, the fire protection materials may suffer from deterioration.

As it will be described later, in 2 out of 11 tests, thermal insulations were also considered on the panel zone of the connection to examine their effects on the fire endurance time of the connection. In the current study, introducing partial thermal insulating of the connection panel zone in specimens S8 and S9 was not aimed at modeling of thermal insulating in a real connection. Partial insulating was introduced to connection components, say separately on the horizontal diaphragms



Figure 5. A view of a specimen during the heating phase.

and vertical stiffeners, to substantiate the importance of these components on the overall fire performance of the connection. The results show that the external diaphragms play a considerably more critical role on the connection fire response as compared to that for the vertical stiffeners.

The third step started when the specimen rotation reached around 200 mrad. The fire was then extinguished in the furnace, and the postfire conditions of the specimen were evaluated. Images were captured during the tests at different temperatures.

### 3. TESTING PROCEDURE

#### 3.1. Test cases

A series of 11 tests were conducted on the aforementioned small-scale I-beam-to-circular tubular leg connections with external diaphragms. All fire tests were carried out under a constant vertical load at the far end of the beam member plus thermal actions until an imminent or actual structural failure limit state was attained, or until a major integrity breach occurred. It is obvious that the higher the applied load, the lower the connection failure temperature will be. The scope of this study was to investigate the behavior of the connection at elevated temperatures. Therefore, the applied moments were selected as a proportion of the ultimate rotational capacity of the connection in room temperature. This was to avoid a premature failure at high temperatures. The flexural capacity ( $M_{cc}$ ) of each connection with external diaphragm can be calculated as follows [37]:

$$M_{cc} = P_{bf} \cdot (h_b - t_{bf}) \quad (4)$$

$$P_{bf} = 19.6 \left( \frac{d_c}{t_c} \right)^{-1.54} \left( \frac{h_d}{d_c} \right)^{0.14} \left( \frac{t_d}{t_c} \right)^{0.34} \left( \frac{d_c}{2} \right)^2 f_{c,y} \quad (5)$$

where  $P_{bf}$  is the axial load in tension or compression flange of beam,  $h_b$  is the beam height,  $t_{bf}$  is the beam flange thickness,  $d_c$  and  $t_c$  are diameter and thickness of tubular column, respectively,  $h_d$  and  $t_d$  are minimum width and thickness of external diaphragm, respectively, and  $f_{c,y}$  is the yield strength of steel column at ambient temperature. The flexural capacity of the connection given by Eqs. 4 and 5, in fact, denotes a moment produced by a pair of tensile/compressive forces in the upper and lower diaphragms. These tensile/compressive forces equal the yielding capacity of an effective width of the diaphragm. In general, Eqs. 4 and 5 appear to imply a full plastic flexural failure mode in the connection diaphragms. However, as these equations are obtained from the curve fittings to the numerical modeling results of the connection, they might implicitly incorporate other failure modes such as local plastic buckling in the compressive flange.

The connection properties in each test, the nominal rotational capacity in each specimen, and the amounts of the applied load are given in Table III. As it can be noticed, some specimens (S1, S3, and S5) were prepared as replicate specimens to ensure repeatability of test results. As it will be reported later, the results of these tests showed high repeatability in terms of the behavior of the connection in elevated temperatures (Table IV). An overall postexperiment view of some specimens is shown in Figure 6.

#### 3.2. Temperature distribution

With all specimens, seven plate thermometers were distributed across the test specimen surface to record the temporal variation of the temperature on different locations/times around the specimens during each test. Data measured by the thermometers at various connection points expectedly showed that temperature did not remain spatially uniform across the specimen. However, the spatial variations were not very significant. Measurements on the temporal/spatial variation of the temperature along the connection will be needed for numerical simulation of the experiment as a future complementary work. The results of the numerical study on the subject are not presented here and will appear in a separate paper. In the current paper, the spatial variation of the temperature

Table III. Thickness for the connection compartment and the applied loads in different specimens.

Specimen number	Thickness of external diaphragm plates (mm)	Thickness of web/stiffener plates (mm)	Moment ( $M$ ) level ( $M_{cc}$ )	Initially applied moment to the specimen (kN·m)	Average moment recorded during the test (kN·m)
S1	12	6	0.4	44.8	44.78
S2	12	6	0.4	44.8	44.85
S3	12	6	0.3	33.6	33.65
S4	12	6	0.2	22.4	22.42
S5	12	6	0.1	11.2	11.28
S6	15	6	0.3	33.6	33.66
S7	12	8	0.3	33.6	33.64
S8	12	6	0.3	33.6	33.55
S9	12	6	0.3	33.6	33.55
S10	12	6	0.3	33.6	33.64
S11	12	6	0.1	11.2	11.24

$M_{cc}$  is equal to the plastic moment capacity of the connection and  $M$  is the applied bending.

Table IV. Objectives and relationships between different test cases.

Specimen number	Objectives/relation between the test cases
S1, S3, S4, and S5	Effect of the moment magnitude on the connection behavior
S3, S6, and S7	Effect of strengthening the external diaphragms
S3, S8, and S9	Effect of insulating the joint panel
S1 and S2	Repeatability control of the tests
S3 and S10	Repeatability control of the tests
S5 and S11	Repeatability control of the tests



Figure 6. Postfire test view of some specimens.

across the specimen was ignored. So, the specimens' responses are reported against the time series of the average temperature, taken from all thermometers employed. As an example, Figure 7 gives the time series of the average temperature recorded in a number of tests. Figure 8 gives sample time series of seven thermometers' records for specimen S3, plus the average temperature for this specimen. The whereabouts of the thermometers are shown in Figure 4.

### 3.3. Rotation calculation

Clinometers and LVDT transducers were used to measure the rotation of the connections tested. The LVDT transducers were basically used to measure the vertical deflection at different positions along the I-beam and the lateral displacement along the tubular column. Their data were used to calculate

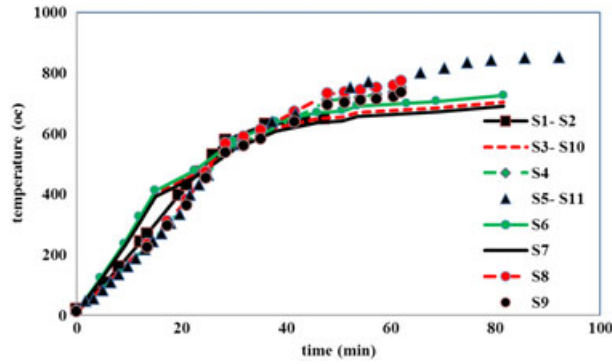


Figure 7. Average temperatures in different specimens.

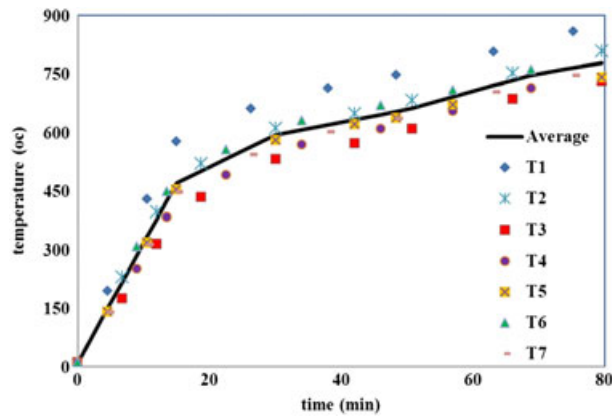


Figure 8. Time series of seven thermometers' records for specimen S3, plus the average temperature for this specimen.

the rotation of the connection. The in-plane rotation,  $\varphi$ , on each of the column and beam components was calculated from LVDT transducer readings. It was calculated from the following equation [38]:

$$\varphi = \tan^{-1}(u/L) \tag{6}$$

where  $u$  was the deflection of the point along the beam/column, and  $L$  was the distance from the connection center axis to the point where deflection was measured. The net rotation of the connection was defined as the difference between the column and the beam rotations. In each test, three LVDTs on top of the beam flange were used to calculate the rotation of the connection. The LVDTs were placed out of the furnace with different spacing from the column axis. The closest LVDT to the connection was used as a reference for the rotation calculation. Readings from the two other LVDTs and inclinometers were used to further verify the rotation calculations and for comparison purposes.

It is noted that in several occasions the inclinometers became unfunctional and burned during the tests. The inclinometer was placed on the beam flange, out of the furnace but very close to furnace wall readings. This was to ensure that they would report the connection rotations. During the furnace calibration tests, the maximum temperature at inclinometer location was estimated for an uninstrumented specimen. The data were then checked against the operating limits provided by the manufacturer.

The inclinometer readings tended to be erratic in a number of early tests. It was judged that the device was experiencing temperatures greater than that recorded for the uninstrumented specimens during the furnace calibration tests. This might be caused by heat radiation coming from the opening

in the furnace wall for the beam penetration. The LVDTs readings were not irregular. For this reason, the joint rotation calculations were based on LVDT measurements, and the inclinometers were abandoned in later tests.

#### 4. RESULTS AND DISCUSSION

The test results in this section present a family of rotation–temperature curves for the examined connections. They provide an insight into the behavior of the welded steel I-beam-to-circular tubular chord connections at elevated temperatures. The configuration of tests considered in this study provided the possibility of investigating effects of certain parameters on structural behavior of the connections at elevated temperatures. The objectives of different test cases and their relationships are summarized in Table IV.

It is noted that fire tests are costly and time consuming. Typically, only a limited number of test cases and few parameters were considered in the experiments. There would be a need for further research to support and to expand the findings of this study. The experimental results are also used for numerical simulation of the experiment, as a complementary work. The numerical study is aimed at extending the study to other I-beam-to-tubular chord connection geometries and will be presented in a separate paper.

##### 4.1. Temperature–rotation responses

It is possible to derive temperature–rotation curves of connection at elevated temperatures using the data measured during the tests. Sample temperature–rotation responses of some specimens are shown in Figure 9. As it can be seen, the temperature–rotation curves of the connections can be classified into three regions. The connection initially demonstrates an almost linear response with increasing temperatures. This is followed by a curved knee response that identifies the yielding or local instability in one or more components in the connection yield. Finally, as the connection failure becomes imminent, the rotation rate rapidly increases indicated by an almost flat plateau in the connection response.

##### 4.2. Effect of the applied load on the connection behavior

Different connections in a real offshore superstructure may carry different bending moments, depending on their whereabouts, configurations, or conditions in the structure. Moments acting on a connection might also experience spatial and temporal variation because of the changes in the load distribution over the interconnecting structural elements. In the current study, the effect of the applied moment magnitude on the fire performance of the I-beam-to-tubular column connections was investigated. As it may be noticed in Table IV, the only difference between specimens S1, S3, S4, and S5 was to their applied moments. The S1 specimen was carrying the maximum applied

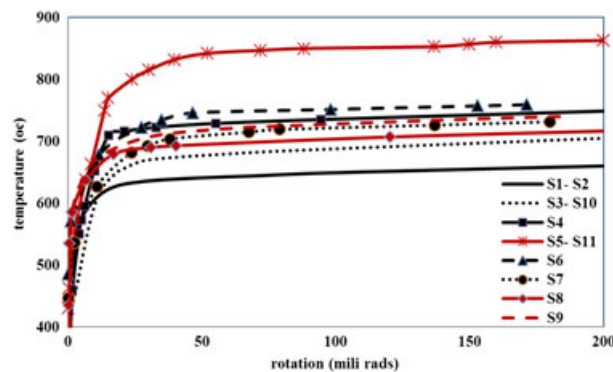


Figure 9. Temperature–rotation responses.

uniplanar bending equal to  $0.4 M_{cc}$ , whereas the S5 specimen was carrying the smallest one ( $0.1 M_{cc}$ ). The applied loads were introduced to the specimens at room temperature and kept constant all through the fire tests. During the fire tests, the specimens were exposed to identical (standard) temperature ramping conditions. Temperature–rotation curves recorded for specimens S1, S3, S4, and S5 during the fire tests are presented in Figure 10.

As it was expected, the connection tolerated higher temperatures with a decrease in the applied moment (Figure 10). However, the effects were nonproportional and highly nonlinear. The temperature corresponding to the total failure of the S5 specimen (with an applied load of  $0.1 M_{cc}$ ) was around 32% higher than that for the S1 specimen (with an applied load of  $0.4 M_{cc}$ ). The effects of the applied load on the connection behavior became more remarkable as the applied load magnitude increases. The results for S1 ( $0.4 M_{cc}$ ) and S3 ( $0.3 M_{cc}$ ) specimens shows that  $0.1 M_{cc}$  increase in the applied load caused around 16% variation to the failure temperature. With specimens S4 ( $0.2 M_{cc}$ ), and S3 ( $0.3 M_{cc}$ ), the same amount of increase in the applied load caused around 6% variation to the failure temperature.

#### 4.3. Effect of strengthening of external diaphragms/stiffeners

Effects of thickening the external diaphragms/stiffeners on the rotational behavior of welded steel I-beam-to-circular tubular chord connections at elevated temperature were also studied. As it can be seen from Table III, the only difference between specimen S3 and specimens S6 and S7 was the thickening of the connection components in the panel zone. With specimen S6, the thickness of the external diaphragms was increased from 12 to 15 mm, whereas the thickness of the stiffeners and other connection properties remained similar to those in S3 specimen. With S7 specimen, the thickness of the stiffeners was increased from 6 to 8 mm, whereas the thickness of the external diaphragms and other connection properties remained similar to those in S3 specimen (Table III). The variations in thicknesses used were arbitrary. All three specimens were examined under identical applied moments equal to  $0.3 M_{cc}$  (see Table III). Temperature–rotation curves for the three mentioned specimens are shown in Figure 11.

As it can be observed from Figure 11, by thickening the external diaphragms in the panel zone the connection thermal capacity was increased and the connection tolerated higher temperatures. The maximum temperature tolerated by the S6 and S7 specimens were around 10% and 5%, respectively, higher than that with the S3 specimen. The strengthening of the panel zone had more profound effects on the connection behavior in temperature ranges from 450 to 650 °C. The rotation–temperature curves for S6 and S7 specimens show a remarkably stiffer behavior in this range of temperature. They also follow smoother paths that are located to the left side (lower nonlinearity in elevated temperature) of that for the S3 specimen. The reason is that the stiffness and strength of a connection is directly related to the stiffness and strength of the connection components. The stiffness and strength of the connection components depend on the elasticity

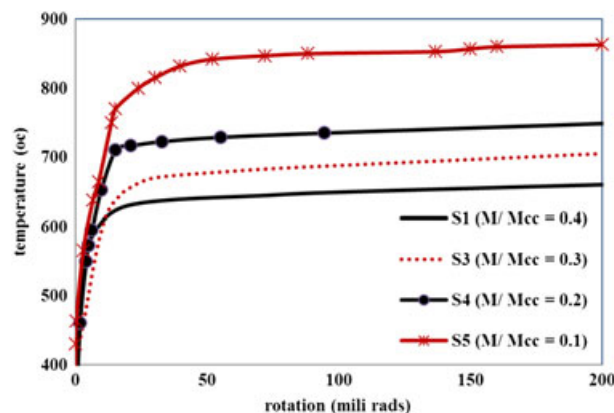


Figure 10. Effect of applied moment magnitude on the temperature–rotation response of the specimens.

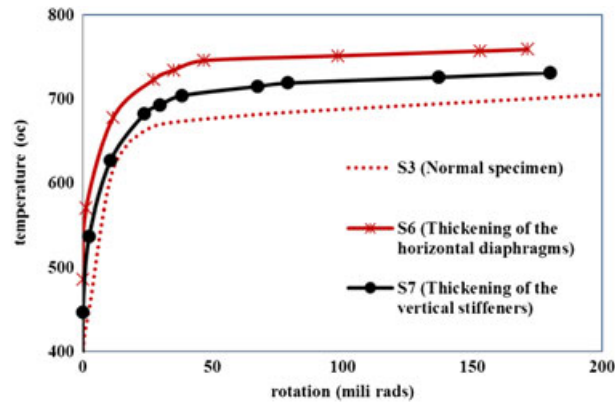


Figure 11. Effect of thickening the external diaphragms/stiffeners on the temperature–rotation response of the specimens.

modulus and load bearing of the steel components by which they are fabricated. By the increase of web/stiffener plate thickness or flange plate thickness in the panel zone, stiffness and load bearing of the connection is increased. The modulus of elasticity and the steel strength deteriorate with temperature increases according to Table V. Complete deterioration of stiffness and strength in a connection with higher stiffness occurs at higher temperatures, and consequently, it can tolerate higher temperatures compared with the temperature that a connection with lower thickness plates can.

As it can be seen in Figure 11, thickening of the external diaphragms had slightly higher effects on the maximum temperature tolerated by the connection as compared with that from thickening of the stiffeners. The reason can be attributed to the fact that the final failure mode in this type of connection at elevated temperature was found to be a local buckling in the compressive external diaphragm. Strengthening of this location postponed the local buckling and the overall failure and is more effective than thickening the stiffener plates.

Then, it should mention that undue strengthening of the panel zone may trigger additional and most undesirable failure mode in the connection. This is a failure in the column instead of the favorable failure in the beam or in the beam-to-column segments of the connection. All connections considered in the current study were designed on the basis of a strong-column/weak-beam criterion. The connection failure under in-plane bending was found to be initiated by local failures either in the vertical stiffeners or horizontal diaphragms in the connection panel zone and not by the failure in the column wall. By strengthening the connection components, the failure mode was transferred from the connection to the column wall. A failure in the column is not desirable because it possibly

Table V. Reduction factors for the stress–strain curves of steel at elevated temperatures [39].

Reduction factors for yield stress $f_y$ , and Young's modulus $E_s$ at steel temperature $\theta_s$		
Steel temperature, $\theta_s$ (°C)	$k_{y,\theta} = f_{y,\theta}/f_y$	$k_{E,\theta} = E_{s,\theta}/E_s$
20	1	1
100	1	1
200	1	0.90
300	1	0.80
400	1	0.70
500	0.78	0.60
600	0.47	0.31
700	0.23	0.13
800	0.11	0.09
900	0.06	0.068
1000	0.04	0.045
1100	0.02	0.023
1200	0	0

causes a brittle failure in the structure. To avoid this failure mode and achieve a ductile response, it is necessary to avoid undue strengthening of the connection components. Alternatively, the column can be locally reinforced by introducing a joint can. This mode of failure was observed in S6 specimen. In addition to other local failures to the external diaphragm and the vertical stiffener, the column segment in the panel zone experienced a noticeable sway deformation at elevated temperatures.

#### 4.4. Effect of partial insulating the panel zone

The endurance time of a steel connection can be increased by delaying the rise in the steel temperature. One of the methods for strengthening steel members against fire is the use of thermal insulations. Then, the temperature rise in a protected steel section depends on the thermal characteristics of the insulation material, its conductivity and thickness, and on the shape factor of the steel profile. External fire protections are frequently used in highly important structures including oil platforms. Different types of external fire protection materials can be considered for this purpose. If external fire insulation is provided, the steel temperature development depends not only on the shape factor but also on the type and thermal performance of the insulation material.

In the current study, the specimens S8 and S9 were selected to investigate the effect of partial external fire protection on the specimen response at elevated temperatures. The geometrical and mechanical properties of these specimens were the same as those in the specimen S3. The only difference was the external fire protection cover used in specimens S8 and S9. With specimen S8, only the vertical stiffener plates in the connection panel were insulated, whereas in specimen S9, only the horizontal external diaphragms were insulated. The fiber ceramic used for the partial thermal insulation of the connection diaphragms/stiffeners was a production of DS Fibertech Corp. The average thermal conductivity of it was 0.15 W/mK. Temperature–rotation curves for these specimens are presented in Figure 12.

The results depicted in Figure 12 show that the use of fireproofing cover increases the connection thermal capacity, as it was anticipated. Results presented in Sections 4.3 showed that thickening the external diaphragms/stiffeners had a more significant effect on the fire performance of the specimens than that from the thermal insulation of the same components. The reason can be attributed to the fact that the thermal insulation covers were only considered on limited areas in the panel zone (for instance, only on external diaphragms or on the vertical stiffeners). The insulated components were able to delay the temperature rise in these components as compared with other areas in the connection panel. Therefore, lower rotations and deformations were produced in these components compared with the adjacent regions in the panel zone. This provision, however, fell short to provide a complete heat seal because of the thermal conductivity through other steel elements present in the connection panel. In the case where no fireproofing cover was used, the temperature was almost simultaneously rising on all parts of the connection.

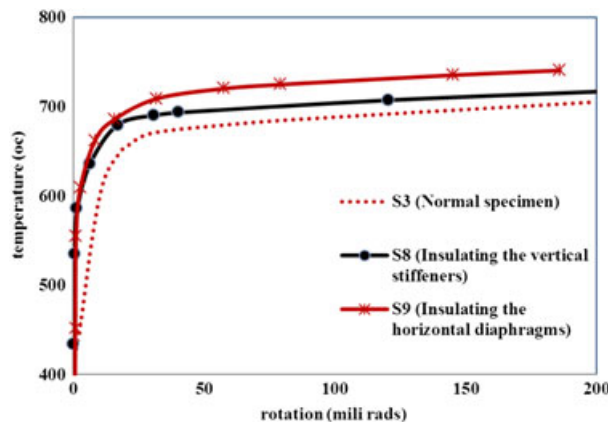


Figure 12. Effects of partial insulating the panel zone on the temperature–rotation response of the specimens.

Considering the aforementioned subjects, it can be concluded that when thermal insulations are considered for fire strengthening the welded steel I-beam-to-tubular chord connections, the panel zone area should be entirely insulated. In this way, all panel zone components temperature distribution will be uniform, the connection acts as a solid member, the interaction between connection components is provided, and each of the connection component has a specific proportion in inducing deformations and other thermal effects. A comparison of effects from thickening the external diaphragms/stiffeners and partial insulating the panel zone on the temperature–rotation response of the specimens is seen in Figure 13.

#### 4.5. Failure modes of the connection

One important feature in the fire response of steel connections is the comprehension of the failure modes of the connection. A designer needs a proper understanding on the failure mechanisms in each structural member to prevent brittle and unpredicted failure in a structure and to replace the failure modes in part of structure with ductile and proper failure modes.

The results of the current fire tests carried out on the welded steel I-beam-to-tubular chord connections showed that the increase in the temperature caused local plastic buckling on the vertical stiffener plates in the panel zone, local buckling in the compressive external diaphragm, yielding failure in the tensile external diaphragm, and finally, tensile tearing in the welds between the I-beam flange and the external diaphragm. Some of these failure modes can be seen in Figure 14. It is noted that the sequence of the aforementioned failure modes varied among different specimens, depending

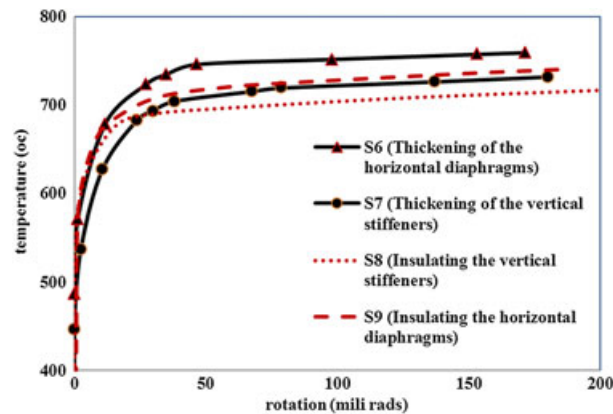


Figure 13. Comparison of the effects of thickening the external diaphragms/stiffeners and partial insulating the panel zone on the temperature–rotation response of the specimens.



Figure 14. Postfire test view of the S4 specimen showing some of the failure mechanisms in the specimen.

Table VI. Relation between the test results and the degradation of material properties together with the failure modes of the different specimens.

Specimen number	Moment ( $M_{cc}$ ) level	Average moment recorded during the test (kN·m)	Failure temperature (°C)	Reduction factors for yield stress at $\theta_s$	Yield stress at $\theta_s$	Classical rotational moment capacity at $\theta_s$ (Eq. 4)	Governing failure mode
S1 and S2	0.4	44.8	633	0.391	138.8	43.79	LPB-CED
S3-S10	0.3	33.65	670	0.302	107.2	33.83	LPB-VSP LPB-CED
S4	0.2	22.42	715	0.212	75.2	23.75	LPB-VSP LPB-CED
S5-S11	0.1	11.28	815	0.103	36.5	11.54	YF-TED LPB-CED
S6	0.3	33.66	727	0.198	70.3	23.93	YF-TED CWF
S7	0.3	33.64	693	0.247	87.7	27.67	LPB-VSP LPB-CED
S8	0.3	33.55	690	0.254	90.17	28.46	YF-TED LPB-CED
S9	0.3	33.55	707	0.222	78.67	24.85	YF-TED CWF LPB-VSP

LPB-CED, local plastic buckling in the compressive external diaphragm; CWF, column wall failure; LPB-VSP, local plastic buckling in the vertical stiffener plates; and YF-TED, yielding failure in the tensile external diaphragm.

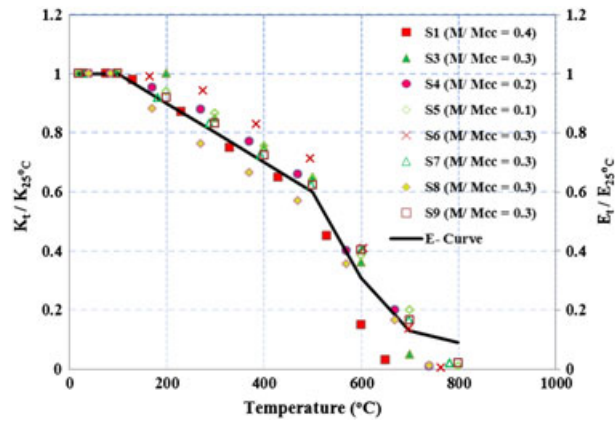


Figure 15. Variations of the nondimensionalized rotational connection stiffness and Young's modulus by temperature.

on the mechanical and geometrical properties of the external diaphragms and the stiffeners, and whether they were insulated or not. The dominant failure mode with specimens S2 and S3 was the local plastic buckling of the compression external diaphragm. This was caused by gradual decreases in the elastic modulus and in the yield stress because of temperature increase. As a result, the threshold stress for local buckling gradually decreased. Consequently, at a specific time (temperature), the threshold stress for local buckling reduced to the compressive stress available in the connection diaphragm. This triggered a local buckling in the compression diaphragm. The local buckling in the external diaphragm was followed by an in-plane shear failure that was then extended to the compressive flange in the I-beam. With specimens S6 and S9, the column showed also noticeable deformations at high temperatures. The dominant failure modes in the different specimens are given in Table VI.

It tried to relate the connection capacity in the fire to the degradation of material properties. The results are presented in Table VI. The table gives the test results for the connection capacity together with the temperature at failure (when the rotation reached 30 mrad). The material yield stress at this temperature was then calculated from [39]. This degraded yield stress was introduced to Eqs. 4 and 5 to obtain an estimate for the connection capacity at elevated temperature. It is noted that these equations were originally giving the theoretical joint capacity at room temperature. Table VI shows a good correlation between the connection capacity from the tests and the estimates obtained from Eqs. 4 and 5. This is true for all specimens except for S6, S7, S8, and S9, where the difference between the tests and the estimates reaches to around 30% (the estimates are conservative). It is noted that specimens S6 to S9 were strengthened either by thickening or insulating of their external diaphragms/stiffeners. These measures resulted in the improvement of the ultimate bending capacity of the connections at elevated temperature but triggered different failure modes such as failures in the column rather than in connecting elements. These types of failure modes, almost certainly, are overlooked in Eqs. 4 and 5.

#### 4.6. Rotational stiffness at elevated temperature

The connection stiffness degrades in fire. At elevated temperatures, even small degradations in connection stiffness will have serious impacts on the overall fire performance of a moment-resisting steel frame. Figure 15 rearranges test results from the current study. It gives the variation of rotational stiffness of the connections against temperature increase. Rotational tangent stiffness of a connection ( $K$ ) is taken as the slope of the moment-rotation ( $M-\theta_r$ ) curve. The connection stiffness at elevated temperatures ( $K_t$ ) is nondimensionalized using the connection rotational stiffness at room temperature (25 °C). The figure also depicts the variation of Young's modulus for the carbon steel materials with temperature on the basis of the Eurocode [39]. The Young's modulus at elevated temperatures ( $E_t$ ) is also nondimensionalized using the Young's modulus at room temperature (25 °C). The latter curve is titled as E-Curve.

Figure 15 shows that at low temperatures, the connection stiffness virtually remained unchanged. It degraded almost linearly when the temperature increased from 100 to around 450 °C. The degradation in the stiffness gathered speeded afterward. As it can be seen in Figure 15, variations of the rotational stiffness at elevated temperature closely followed the E-Curve, in particular prior to 600 °C. It indicates that the connections' stiffness at elevated temperature might be well approximated by using the classical thermomechanical data on steel material.

## 5. CONCLUSIONS

Fire occurrence is one of the greatest threats to oil/gas offshore platforms. Fire accidents in offshore facilities may lead to partial or total collapse or sinking of an offshore platform with serious consequences including loss of lives, destruction of properties, and damages to the environment. Thus, it is vital to ensure that an offshore oil and gas structure is properly designed to minimize the postaccident consequences if a fire does happen to the structure. The present paper focused on the behavior of the welded I-beams-to-tubular connections with external diaphragms, commonly used in the topside of offshore structures, at elevated temperatures. An experimental approach was considered.

Eleven small-scale experimental tests were conducted on uniplanar welded steel I-beam-to-tubular chord connections to investigate their fire performance. Specimens considered in the current study were constructed to 1/8 scale of an existing connection in the main deck of a real platform. The tests were conducted in a gas-fired furnace that was specifically designed for this study. The specimens were first subjected to a predefined applied uniplanar bending in room temperature. The specimens were then exposed to gradually increasing temperature until the specimens failed under combined actions of the applied load and elevated temperatures.

The fire test results were presented as a family of temperature–rotation curves. Effects of multiple parameters on the behavior of these connections and their failure mechanisms at elevated temperatures were studied. They included the applied moment magnitude, thickening the horizontal diaphragms or the vertical stiffeners, and partial thermal insulating of the panel zone.

As expected, with a decrease in the applied moment, the connection was tolerating higher temperatures. However, the effects were nonproportional and highly nonlinear. With thickening of either the connection external diaphragm or the vertical stiffeners, the thermal capacity of the connection was fairly increased. Thickening of the external diaphragms had a slightly higher effect on the thermal capacity of the connection as compared with that from thickening of the vertical stiffeners. Nevertheless, thickening of either external diaphragm or the vertical stiffeners noticeably affected the rotational stiffness of the connection. This was more profound in 450 to 650 °C temperature ranges, where the rotational stiffness of the strengthened connections were several times higher than that for the normal design. Effect of partial thermal insulating (of either the external diaphragm or the vertical stiffeners) was also studied. Partial insulation had some increasing effects on the thermal capacity of the connection. But, thickening the external diaphragms/stiffeners was more effective on the thermal capacity than thermal insulation of the same component. Partial insulation of the connection diaphragms/stiffeners had also an increasing effect on the rotational stiffness of the connection in particular in 450 to 650 °C temperature ranges.

The temperature rise was causing a succession of failure mechanisms in the connection. They included local plastic buckling in the vertical stiffener plate, local plastic buckling in the compressive external diaphragm, yielding failure in the tensile external diaphragm, and tensile tearing in the welds between the I-beam flanges and the diaphragms. The sequence of the failure mechanisms varied among different specimens, depending on the thickness of the external diaphragms and the stiffeners, and whether they were insulated or not. With some specimens, a failure mode in the column prevailed the aforementioned failure mechanisms. This appeared to be caused by extra strengthening of the panel zone elements in those specimens. In the cases S6 and S9, although an improved connection capacity was achieved by strengthening the external diaphragms, the failure mode was transferred from the connection elements to the column, which is highly undesirable. To preclude this undesirable failure mode and to achieve a ductile response, it is therefore important to avoid undue strengthening of the connection components. Alternatively, the column can be locally reinforced by introducing a joint can.

It is noted that the results presented in this study were obtained from a limited number of small-scale tests. There is, therefore, a need for further research to support and to expand the findings of this study. The results of this study are expected to be useful for other investigations about the behavior of connections in fire, particularly for creating and validating the numerical models because there are few experimental tests in this area.

## ACKNOWLEDGEMENTS

The authors wish to acknowledge IOEC for providing the material, fabricating the specimens, and the quality control tests, Mr. Changizi from ETA company for manufacturing the furnace and providing the fire test facilities, Dr. Yahyai and Mr. Ahmadi from K. N. Toosi University, for providing the instrumentations and data acquisition devices, POGC for partial financial support of the study, and Dr. Bahaari from IOEC and Dr Daghigh for their constructive advice and suggestions.

## REFERENCES

1. Zeinoddini M. *Design and Construction of Offshore Oil Platforms*. Iranian Oceanography Institute; 2005 (In Persian).
2. Zeinoddini M, Parke GAR, Harding JE. Interface forces in laterally impacted steel tubes. *Proceedings of the Society for Experimental Mechanics, Inc.* 2008; **65**:265–280.
3. Amdahl J. Ultimate strength. Technical committee III. In *Proceedings of the 14th International Ship and Offshore Structures Congress*. Vol. 1, Ohtsubo H, Sumi Y (eds). Elsevier: Nagasaki, Japan, 2000; 253–321.
4. Sandrea I, Sandrea R. Growth expected in global crude oil supply. *Oil and Gas Journal* 2007; **105**(10):34.
5. DNV. Accident statistics for fixed offshore units on the UK continental shelf 1980–2005, Statistics reports. Prepared by Det Norske Veritas for the Health and Safety Executive, UK, 2007.
6. WOAD. Worldwide offshore accident databank. Det Norske Veritas. Oslo, published biannually. 2008.
7. Health and Safety Executive. Offshore accident/incident statistics reports, London, UK 2007.
8. Tuhaijan SNAB, Kurian VJ, Mohd SL. Wave-current interaction on offshore spar platforms. In *National Postgraduate Conference (NPC), IEEE*, 2011; 1–5.
9. Khan FI, Amyotte PR. Inherent safety in offshore oil and gas activities: a review of the present status and future directions. *Journal of Loss Prevention in the Process Industries* 2002; **15**:279–289.
10. Wang YF, Xie M, Ng KM, Habibullah MS. Probability analysis of offshore fire by incorporating human and organizational factor. *Ocean Engineering* 2011; **38**:2042–2055.
11. NIST. Final report on the collapse of the World Trade Center Towers. Report NIST NCSTAR 1, National Institute of Standards and Technology, Gaithersburg Maryland (USA) 2005.
12. Beyler CL, Beitel J, Iwankiw N, Lattimer B. Fire resistance testing for performance-based fire design of buildings. *NIST GCR 07–971*, 2007; 154.
13. Strejcek M, Wald F, Reznicek J, Tan KH. Behaviour of column web component of steel beam-to-column joints at elevated temperatures. *Journal of Constructional Steel Research* 2011; **67**:1890–1899.
14. El-Housseiny OM, Abdel Salam S, Attia GAM, Saad AM. Behavior of extended end plate connections at high temperature. *Journal of Const Steel Res* 1998; **46**(1–3):299.
15. Liu TCH. Moment–rotation–temperature characteristics of steel/composite connections. *Journal of Structural Engineering* 1999; **125**(10):1188–97.
16. Mao CJ, Chiou YJ, Hsiao PA, Ho MC. Fire response of steel semi-rigid beam column moment connections. *Journal of Constructional Steel Research* 2009; **65**:1290–1303.
17. Rahman R, Hawileh R, Mahamid M. The effect of fire loading on a steel frame and connection. In *High-Performance Structures and Materials II*, Brebbia CA, de Wilde WP (eds). WIT Press: St Lodge, Ashurst, Southampton SO40 7AA, UK, 2004; 307–16.
18. Saedi Daryan A, Yahyai M. Behavior of bolted top-seat angle connections in fire. *Journal of Constructional Steel Research* 2009(a); **65**:531–541.
19. Saedi Daryan A, Yahyai M. Modeling of bolted angle connections in fire. *Fire Safety Journal* 2009(b); **44**:976–988.
20. Everett EG, Nehring G. An approach to fire control in offshore operations in the North Sea. *Eighth Annual Offshore Technology Conference 1976 Proceedings*. Offshore Technology Conference; Dallas, TX (USA), 1976; 2:405–416 OTC-2558.
21. Soares CG. Probabilistic modelling of offshore fires. *Fire Safety Journal* 2000; **34**:25–45.
22. Eberg E, Amdahl J, Holmas T, Hekkelstrand B. Integrated Analysis of Offshore Structures Exposed to Fire. *1st International Conference and Exhibition, Offshore Structural Design against Extreme Loads*: London, 1992.
23. Shetty NK, Soares CG, Thoft-Christensen P, Jensen FM. Fire safety assessment and optimal design of passive fire protection for offshore structures. *Reliability Engineering and System Safety* 1998; **61**(1):139–149(11)
24. Eberg E, Holmas T, Amdahl J, Landro H, Ulfsnes M. Integrated Fire Analysis of Offshore Structures-Development and Verification of Analysis Procedures. *ERA Technology Conference: Offshore Structures - Hazards, Safety and Engineering*: London, 1995.
25. Arajo MS, Rodriguez SH, Mendes MF, Mansur W. 10 years of computational fire simulation at offshore installations: results, benefits and New developments. *Proceeding of the Ninth International Offshore and Polar Engineering Conference, Brest, France*; 1999.

26. Amdahl J, Holmas T. Ultimate Strength of Structural Members with Attachment During Accidental Fires. *International Conference on Response of Structures to Extreme Loading*. Toronto, Canada; 2003.
27. Holmas T, Amdahl J. *Fire Resistance of Offshore Structures, IV European Conference on Computational Mechanics*. Palais des Congres: Paris, France, 2010.
28. Wang M, Perricone J, Chang CP, Quintiere GJ. Scale modeling of compartment fires for structural fire testing. *Journal of Fire Protection Engineering* 2008; **18**:223
29. Wang M. Scale modeling of structural behavior in fire. Phd thesis. University of Maryland, College Park (USA), 2006.
30. IOEC. Welding procedures for topside connections in foroozan and esfandiar oil fields development project. *Iranian Offshore Engineering and Construction Company (IOEC)*, 2011.
31. Hosseini SA. Fire effects on behaviour of welded steel I-beam to circular tubular chord connections in oil platform decks. PhD thesis. Tehran (Iran): K.N. Toosi University, 2012.
32. Beyler CL, Beitel J, Iwankiw N, Lattimer B. Fire resistance testing for performance-based fire design of buildings. *NIST GCR 07-971*, 2007; 154.
33. ISO 834. Fire resistance tests – elements of building construction, 2002.
34. ASTM- E 119 – 05a. Standard test methods for fire tests of building construction and materials, 2003.
35. Underwriters Laboratories Inc. *UL 1709, Rapid rise fire tests of protection materials for structural steel*, 4th Edition, Underwriters Laboratories Inc. (UL): Northbrook, IL, USA, 2011.
36. EN 1363-2. Fire resistance tests – part 2: alternative and additional procedures, Brussels. 1999.
37. Kamba T. Study on deformation behaviour of beam-to-CHS column connections with external diaphragms. *Research Report*, Kinki Branch of Architectural Institute of Japan, Osaka, Japan, (in Japanese), 2001; **41**:201–204.
38. Yahyai M, Saedi Daryan A. The study of welded semi-rigid connections in fire. *The Structural Design of Tall and Special Buildings* 2011. DOI: 10.1002/tal.727.
39. Euro code 3. Design of steel structures, part 1.2: general rules structural fire design, prEN-1993-1-2. *European Committee for Standardization (CEN)*; 2003.